Supporting Information

Dagliyan et al. 10.1073/pnas.1218319110

SI Materials and Methods

DNA Construction. All restriction enzymes were purchased from New England Biolabs. All site-directed mutagenesis and gene insertion experiments were performed with the QuikChange mutagenesis kit (Stratagene). PCR products were used as megaprimers for QuikChange mutagenesis reactions (Table S1). The uniRapR domain was created by using PCR such that the 5′- and 3′-end sequences anneal at the desired insertion site within the Src, focal adhesion kinase (FAK), and p38 constructs.

Modeling of uniRapR and Src-uniRapR Structures. To model uniRapR, we removed the first 20 residues from FKBP12 [Protein Data Bank (PDB) ID code 1FAP] by using PyMol (www.pymol.org), so that the two termini are close in space for insertion. We built a circularly permuted FRB by excising at Asn2093 and joining the N- and C-termini together. We removed first four unstructured residues of FRB and connected the two termini with a peptide linker (PPGPGSG). To build a single-chain protein, we excised FKBP12 in Pro88 and connected FRB-G2092 to FKBP12-Gly89 and FKBP12-His87 to FRB-Val2094 with corresponding linkers (Fig. S2). We optimized the complex structure by minimizing the energy by using all-atom discrete molecular dynamics (DMD) simulations. We kept the unmodified regions of FKBP12 and FRB molecules static, whereas linkers were allowed to move to sample conformation and form peptide bonds under the peptide bond constraints between FKBP12/FRB and linkers.

Similarly, we modeled Src-uniRapR by excising the catalytic domain of Src at peptide bond of N287-G288 (PDB ID code 1Y57) and joining the termini of Src insertion loop and uniRapR with corresponding linkers, GPG. We used the model structures after energy minimization to perform replica-exchange simulations to characterize the folding thermodynamics or constant temperature simulations to probe the conformational dynamics. To model the rapamycin-bound state, we applied constraints (Table S2) between rapamycin and subdomain-A similar to interactions of rapamycin with FKBP12 in the crystal structure.

Computational Analysis of uniRapR. We performed all-atom DMD simulations to study the conformational dynamics of uniRapR. A complete description of the DMD algorithm can be found elsewhere (1, 2). We performed replica-exchange DMD simulations to estimate the folding thermodynamics. We used 18 replicas with temperatures ranging from 0.52 kcal/mol·k_B (~260 K) to 0.75 kcal/mol·k_B (~390 K), with an increment of 0.02 kcal/mol·k_B (0.01 kcal/mol·k_B between 0.64 kcal/mol·k_B and 0.72 kcal/mol·k_B). The length of each simulation is 1×10^6 time units (~50 ns). We applied the weighted histogram analysis method to estimate thermodynamic properties of the uniRapR domain. Next, we computed the partition function, $Z = \int \rho(E) exp(-E/k_B T) dE$, which allowed us to derive the specific heat at different temperatures. We also calculated rmsd and tail distance of subdomain-A as function of temperature by using weighted histogram analysis.

We performed a constant temperature simulation of Src-uniRapR at 0.5 kcal/mol·k_B. This is below the folding transition temperature of uniRapR; therefore, the inserted domain stays folded whereas the DMD simulation optimizes its relative orientation with respect to Src. We computed distances between centers of masses of uniRapR subdomains for multiple trajectories. Similar to subdomain-A insertion into subdomain-B, we applied peptide bond constraints to insert uniRapR into Src kinase and performed equilibrium DMD simulations. We computed normalized dynamic correlation matrices (4) to determine the Src activation mechanism. To exclude protein drift when computing residues' fluctuations correlations and root mean square fluctuations, we translated the center of mass of the protein to the origin and aligned each snapshot with respect to the average structure.

Immunoprecipitation and in Vitro Kinase Assay. Anti-myc and anti-FLAG antibodies were purchased from Millipore and Sigma, respectively. Anti–phospho-paxillin-pTyr31 and anti-GFP (JL8) antibodies were purchased from Biosource and Clontech, respectively. Anti–phospho-ATF2 was purchased from Santa Cruz. Rapamycin was purchased from Sigma. Radioactive ATP was purchased from MP Biomedical (7,000 Ci/mmol). Poly-Glu-Tyr (4:1) peptide (E4Y) was purchased from Sigma. HEK293T cells were transfected with 2 μg of DNA constructs by using Fugene6 reagent (Roche). Cells were treated with rapamycin or an equivalent volume of ethanol (solvent of rapamycin solution). Cells expressing Src or FAK constructs were then washed with cold PBS solution and lysed with 20 mM Hepes-KOH, pH 7.8, 50 mM KCl, 100 mM NaCl, 1 mM EGTA, 1% Nonidet P-40, 1 mM NaF, 0.1 mM Na_3VO_4, and Roche protease inhibitor mixture. Cells expressing p38 were lysed with 20 mM Tris, pH 7.5, 150 mM NaCl, 1 mM EGTA, 1 mM EDTA, 1% Triton X-100, 0.5% Nonidet P-40, 20 mM NaF, 0.2 mM Na_3VO_4, and Roche protease inhibitor mixture. Cells treated with rapamycin were lysed with the appropriate lysis buffer containing the corresponding rapamycin concentration. Cleared lysates were incubated with protein G beads attached to anti-myc (for Src and FAK) or anti-FLAG (for p38) antibody for 2 h. The beads were washed three times with wash buffer (20 mM Hepes-KOH, pH 7.8, 50 mM KCl, 100 mM NaCl, 1 mM EGTA, 1% Nonidet P-40) and then with kinase buffer (25 mM Hepes-KOH, pH 7.5, 5 mM $MgCl_2$, 0.5 mM EGTA, 0.005% BRIJ-35) for Src and FAK assays. For p38 assays, beads were washed with p38 lysis buffer and then with p38 kinase buffer (25 mM Hepes-KOH, pH 7.4, 10 mM $MgCl_2$, 25 mM β-glycerophosphate, 4 mM DTT, 0.1 mM Na_3VO_4). For Src and FAK assays, 20 μL of bead suspension were used in the presence of purified substrate paxillin (0.05 mg/mL) and cosubstrate ATP (0.1 mM). For p38 assays, 1 μg purified ATF2 and ATP (0.5 mM) in 40 μL of kinase buffer were mixed with bead suspension for the reaction.

To obtain reaction kinetics, we measured the activity of Src-uniRapR at different time points to determine initial velocities with varying peptide (E4Y) and ATP concentrations (5). We performed the assay as described in the protocol for the Src Kinase Assay Kit (Upstate Biotechnology). At each rapamycin concentration, we titrated the peptide substrate at fixed ATP concentrations. The reaction temperature was at 30 °C. The reaction was stopped with 0.75% phosphoric acid. The phosphorylated substrate was separated from residual [γ-^{32}P]ATP using P81 phosphocellulase paper. The bound radioactivity was quantified with a 1214 RackBeta scintillation counter (LKB).

Live Cell Imaging. HeLa cells were plated on fibronectin-coated coverslips (10 mg/mL fibronectin for 1 h at 37 °C; Sigma) and incubated for 3 h. in DMEM supplemented with 10% (vol/vol) FBS. Then DMEM was replaced with L-15 imaging medium (Invitrogen) supplemented with 5% (vol/vol) FBS. An open heated chamber (Warner Instruments) was used to maintain the cells. Live cell imaging was performed with an Olympus IX-81 microscope equipped with a ZDC focus drift compensator. Images were collected by using a Photometrics CoolSnap ES2 CCD

camera (Roper Photometrics). Metamorph software (Molecular Devices) was used to control the microscope and to acquire and process images at each time point. To calculate cell area, each cell was manually traced around its edge, and a binary mask was created by using Metamorph. Values were normalized to be 1 at the time point before addition of rapamycin.

Imaging of Live Zebrafish. Approximately 5 nL of a DNA–RNA solution containing 20 ng/μL circular DNA of a transposon-donor plasmid and 40 ng/μL transposase mRNA were injected into one-cell zebrafish embryos. Twenty-four hours after the injection, individual embryos with epidermal expression of Src were imaged before and after 16 h of exposure to 10 μM rapamycin (Invitrogen) or vehicle (DMSO). Only epidermal cells with characteristic flat honeycomb morphology were selected for analysis because robust transgene expression induces cell defects before treatment. Imaging was performed on a confocal microscope (FluoView FV1000; Olympus).

1. Dokholyan NV, Buldyrev SV, Stanley HE, Shakhnovich EI (1998) Discrete molecular dynamics studies of the folding of a protein-like model. *Fold Des* 3(6):577–587.
2. Ding F, Tsao D, Nie H, Dokholyan NV (2008) Ab initio folding of proteins with all-atom discrete molecular dynamics. *Structure* 16(7):1010–1018.
3. Kumar S, Bouzida D, Swendsen RH, Kollman PA, Rosenberg JM (1992) The weighted histogram analysis method for free-energy calculations on biomolecules. 1. The method. *J Comput Chem* 13(8):1011–1021.
4. Sharma S, Ding F, Dokholyan NV (2007) Multiscale modeling of nucleosome dynamics. *Biophys J* 92(5):1457–1470.
5. Cole PA, Burn P, Takacs B, Walsh CT (1994) Evaluation of the catalytic mechanism of recombinant human Csk (C-terminal Src kinase) using nucleotide analogs and viscosity effects. *J Biol Chem* 269(49):30880–30887.
6. Yin SY, Ding F, Dokholyan NV (2007) Eris: An automated estimator of protein stability. *Nat Methods* 4(6):466–467.
7. Ding F, Yin SY, Dokholyan NV (2010) Rapid flexible docking using a stochastic rotamer library of ligands. *J Chem Inf Model* 50(9):1623–1632.
8. Suel GM, Lockless SW, Wall MA, Ranganathan R (2003) Evolutionarily conserved networks of residues mediate allosteric communication in proteins. *Nat Struct Biol* 10(3):59–69.

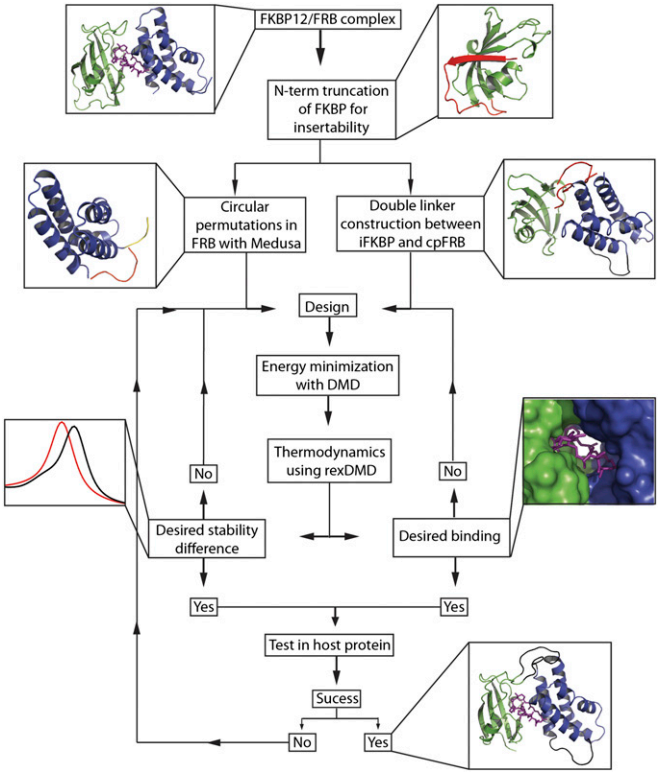

Fig. S1. Design protocol. Two proteins interact in the presence of ligand are chosen as a template structure, such as FKBP (green)/rapamycin (magenta)/FRB (blue) complex (PDB ID code 1FAP). To obtain an insertable design, termini should be close to each other. In this study, for minimal perturbation, we selected a β-sheet hairpin at the C terminal of FKBP12 by removing the first 20 residues. To make a chimeric protein making a hinge motion with a double linker, several designs that include circular permutations of FRB and FKBP linked with different lengths of linkers are considered. These designs are built by using Medusa (6, 7) and DMD by first keeping the domains fixed and allowing the linkers flexible. After energy minimization with all-atom DMD simulations, replica exchange DMD simulations are performed to obtain thermodynamic properties of the designs. If there is a difference in stability in the presence of ligand compared with absence of the ligand, the design is kept. Also, if two subdomains of the design bind to each other only in the presence of ligand, the design is kept. In the case of success, next step is to test switch behavior in a host protein. The insertion site for the designed switch can be determined with our cross-correlation analysis (4) or any other method (8) that provides allosterically coupled sites. A distant site that is allosterically coupled to catalytic site or cosubstrate binding site, i.e., ATP binding site, can be selected for the switch insertion. If the control of host activity that is caged with the designed switch is not robust, a different length of double linker can be used. For example, in the p38 case, the control is more robust if uniRapR is inserted without the default GPG linker.

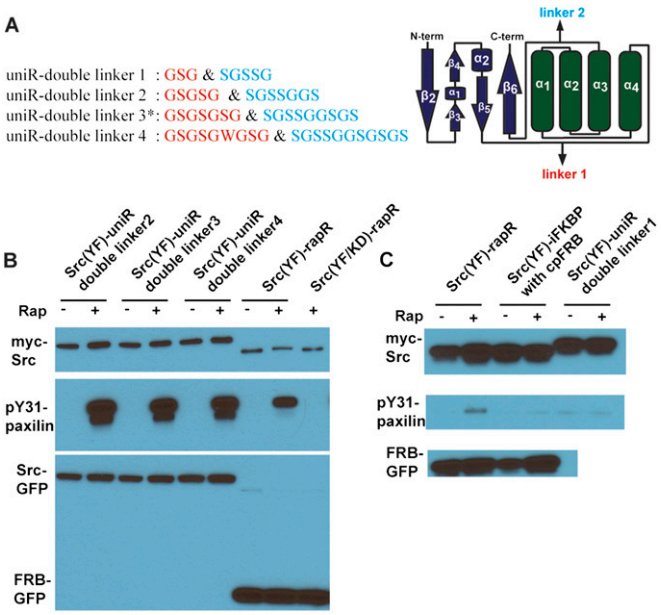

Fig. S2. Testing different lengths of double linkers between uniRapR subdomains. (*A*) Double linker connecting the subdomains-A and -B are shown in red and cyan. The linker with asterisks is the one used in the current version of uniRapR. (*B*) Src-uniRapR-cerulean-myc constructs were expressed in HEK293T cells. Cell lysates were blotted with anti-GFP to confirm the expression of the construct. In dimerization-based switch (rapR), coexpressed FRB was also tested with anti-GFP. Cell lysates were pulled down with anti-myc and mixed with substrate paxillin in the presence of ATP for 10 min. Reaction suspension was blotted with anti-myc to confirm the binding, with anti–pY31-paxilin to confirm the phosphorylation of the substrate. Linker 2 is the one required for functional uniRapR. (*C*) The design with truncated linker 2 (linker 1) does not provide control over Src.

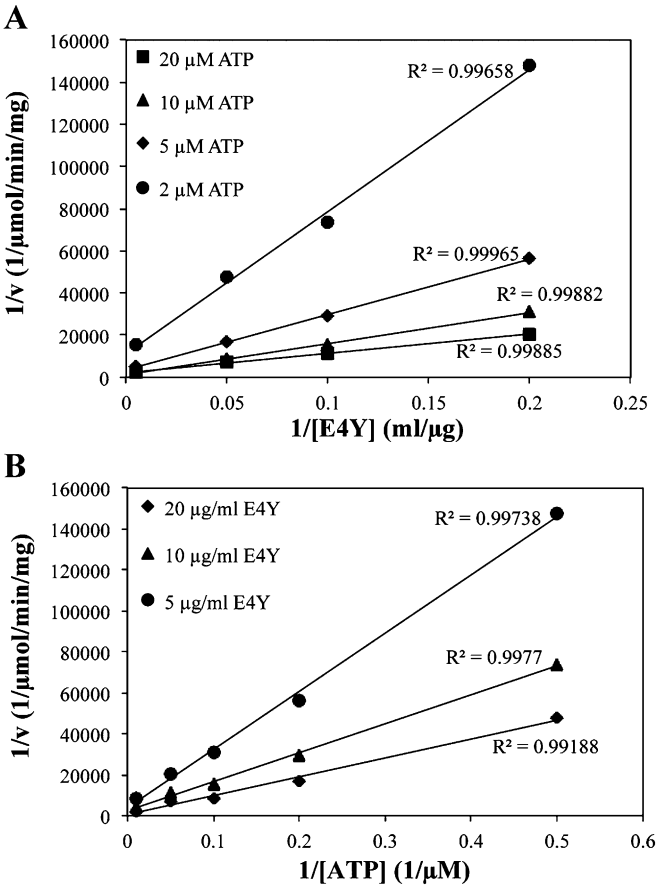

Fig. S3. Substrate kinetics analysis of Src-uniRapR. (*A*) Plot of 1/velocity versus 1/[E4Y] at four fixed ATP concentrations. (*B*) Plot of 1/velocity versus 1/[ATP] at three fixed E4Y concentrations.

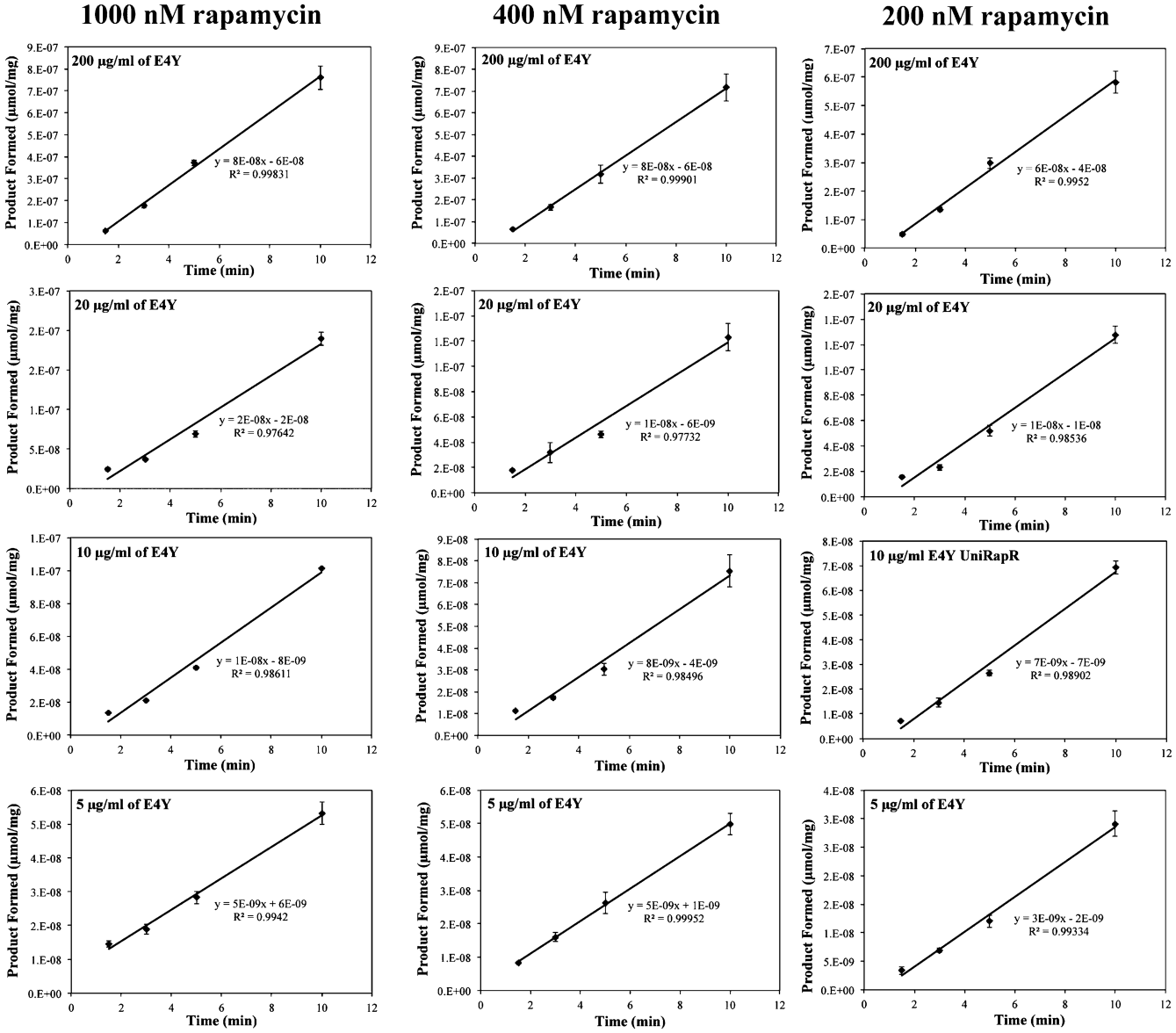

Fig. S4. Velocity of Src-uniRapR at various peptide concentrations (5–200 µg/mL) and rapamycin concentrations (200–1,000 nM).

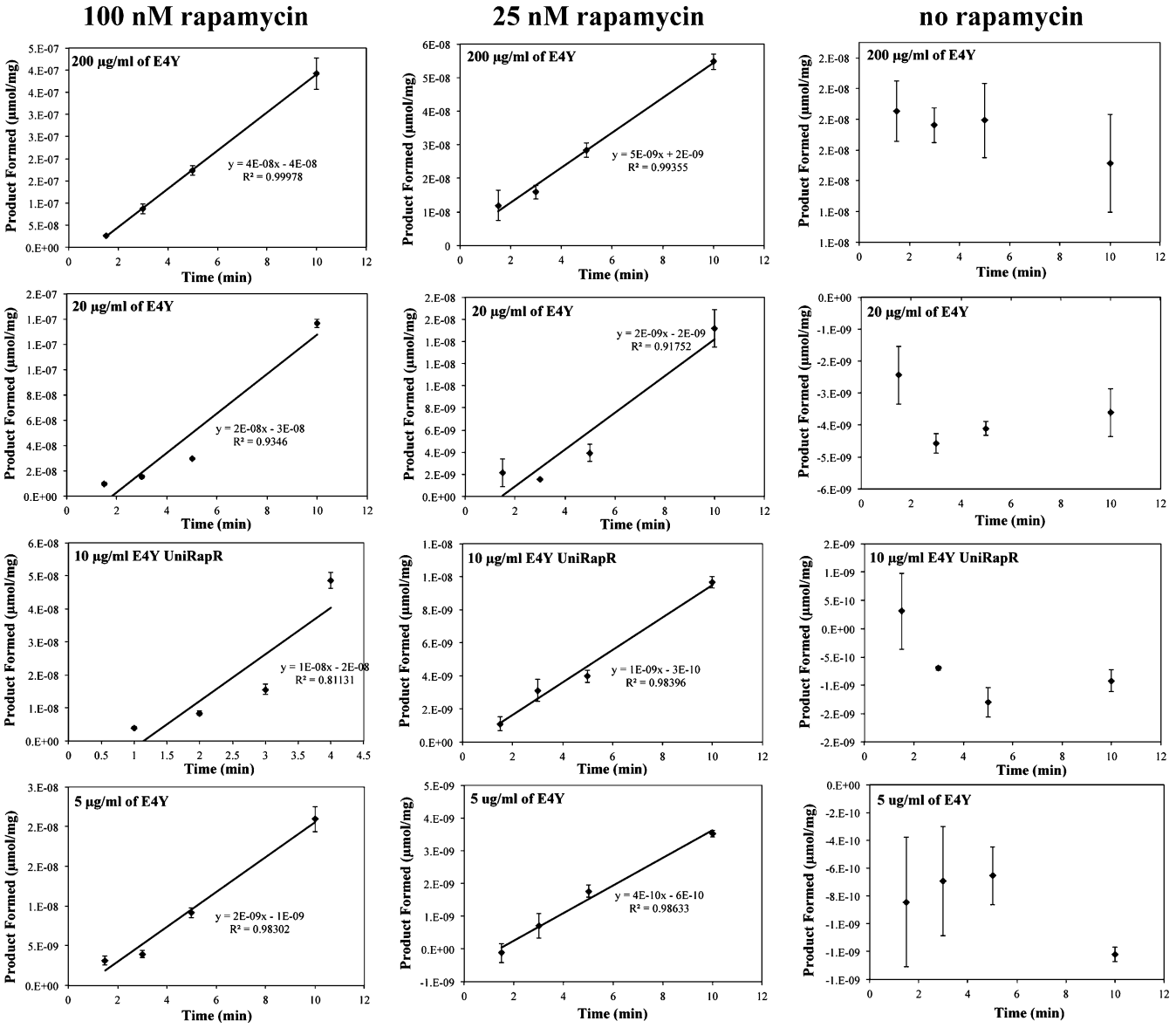

Fig. S5. Velocity of Src-uniRapR at various peptide concentrations (5–200 µg/mL) and rapamycin concentrations (0–100 nM).

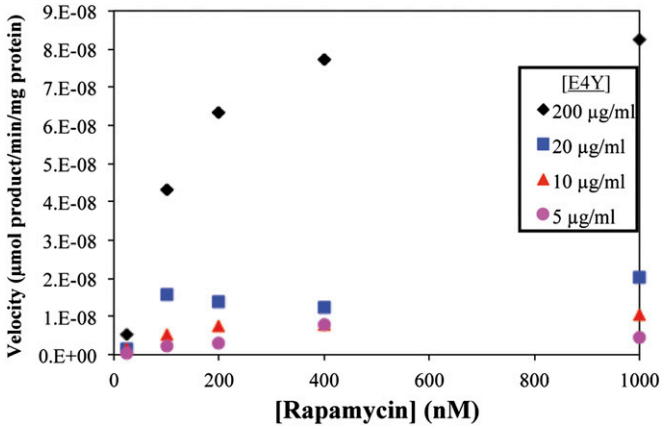

Fig. S6. Rapamycin-dependent velocity profile of Src-uniRapR.

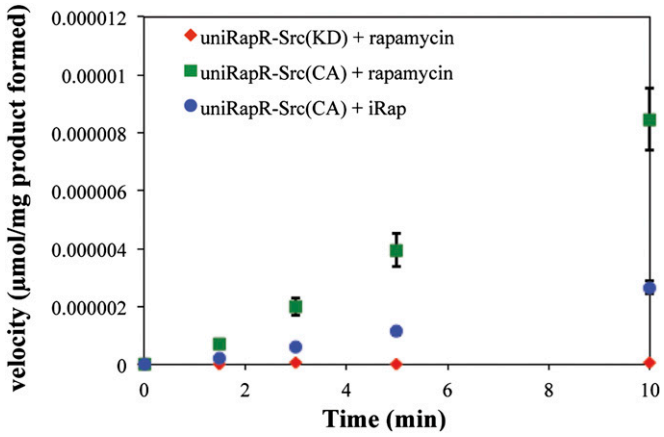

Fig. S7. The velocity of Src (CA)-uniRapR, Src(KD)-uniRapR in the presence of rapamycin, and nonimmunosuppressive rapamycin analogue *iRap*.

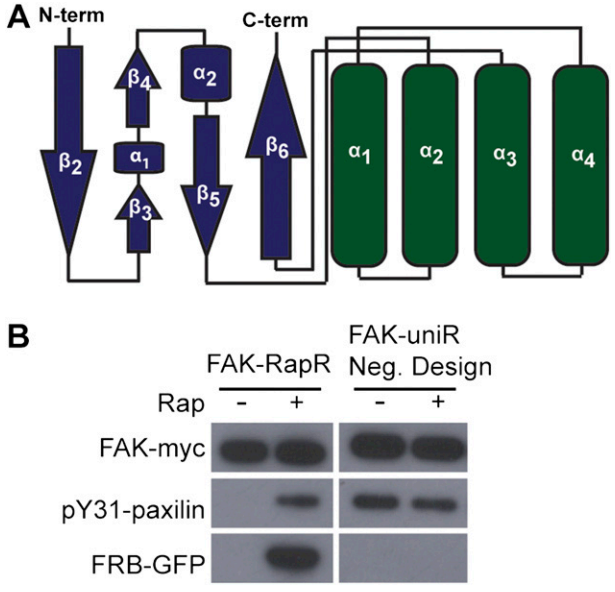

Fig. S8. A different design with different connections between secondary structure components (*A*) does not provide any control over FAK (*B*).

Table S1. Primers used for PCR

Description	Primer sequence (5′ to 3′ forward and 5′ to 3′ reverse)
To replace α4 helix with SSG in FRB	gtgcaggaagtacatgaaatcagggtcatcagggtaaccgtacgacgtaccagactacg
	cgtagtctggtacgtcgtacggttaccctgatgaccctgatttcatgtacttcctgcac
To get megaprimer for cpFRB	Ctcagatctcgagctcaagcttcgaattcagtcaaggacctcctccaagcctggg
	caggccttcatgccacatctcatgccagagacctgatccaggtcctggaggacctgagattcgtcggaacacatgataatagag
To get megaprimer for Src-uniRapR-double-linker1	Ccagattatgcctatggtgccactgggcacggatcaggcgtcaaggacctcctccaagcc
	gacgagagtggcatgtggtgggatgatgccccctgatgaccctgatttcatgtac
To convert double-linker1 to double-linker2	gattatgcctatggtgccactgggcacggttcgggatcaggcgtcaaggacctcctc
	gacgagagtggcatgtggtgggatgattccggagcccccctgatgaccctgatttcatg
To convert double-linker1 to double-linker3	gattatgcctatggtgccactgggcacggttcgggctccggatcaggcgtcaaggacctcctc
	gacgagagtggcatgtggtgggatgatgcctgatccggagcccccctgatgaccctgatttcatg
To convert double-linker1 to double-linker4	gattatgcctatggtgccactgggcacggttcgggctccgggtggggatcaggcgtcaaggacctcctc
	gacgagagtggcatgtggtgggatgatccccgagcctgatccggagcccccctgatgaccctgatttcatg
To convert linker1 to polyProline linker of double-linker3	gattatgcctatggtgccactgggccccctccgccacccccacctccggtcaaggacctcctccaagcctg
	caggcttggaggaggtccttgaccggaggtgggggtggcggaggggggcccagtggcaccataggcataatc
To convert linker2 to poly-proline linker of double-linker3	gagtggtgcaggaagtacatgaaaccaccgccacctccgccacctccaccgccaatcatcccaccacatgccactctcg
	cgagagtggcatgtggtgggatgattggcggtggaggtggcggaggtggcggtggtttcatgtacttcctgcaccactc
Y271A (Y82A in original FKBP12 sequence)	gactatatctccagattatgccgctggtgccactgggcacggttcg
	cgaaccgtgcccagtggcaccagcggcataatctggagatatagtc
Src kinase dead mutation (D388R)	cggatgaactatgtgcaccggcgccttcgagccgccaatatcc
	ggatattggcggctcgaaggcgccggtgcacatagttcatccg
To insert uniRapR into FAK (F442-8 GPG)	cagtttggagatgtacatcaaggcgtgtacggcccaggaacctgcgtggtgcactacacc
	gtttttacatgttttgattgcaacagccaaacctgggccttccagttttagaagctccac
FAK kinase dead mutation (K454R)	ccagctttggctgttgcaatcagaacatgtaaaaactgtacttcgg
	ccgaagtacagtttttacatgttctgattgcaacagccaaagctgg
To insert uniRapR into P38 (PE)	gcctatggctcggtgtgtgctgcttttgatacatacctgagcccaggcacctgc
	cgacagcttcttaactgccacacgatgccccgtcaaagctggattgccttccag

Table S2. Atom pair constraints between C_β atom subdomain B and rapamycin

Subdomain B residue	Corresponding FRB residue in 1FAP	Rapamycin atom index	dmin, Å	dmax, Å
K76	K2095	C14	9.09	11.11
T79	T2098	C14	5.22	6.38
T79	T2098	C16	5.13	6.27
T79	T2098	C10	6.66	8.14
W82	W2101	C16	4.50	5.50
W82	W2101	C18	4.14	5.06
W82	W2101	C20	4.50	5.50
D83	D2102	C16	5.76	7.04
D83	D2102	C18	6.12	7.48
Y86	Y2105	C18	4.14	5.06
Y86	Y2105	C20	3.51	4.29
Y86	Y2105	C23	4.95	6.05
F89	F2108	C21	5.13	6.27
F89	F2108	C23	4.14	5.06
F89	F2108	C25	6.03	7.37
L111	L2031	C23	4.86	5.94
L111	L2031	C25	6.93	8.47
L111	L2031	C21	6.03	7.37
E112	E2032	C22	5.94	7.26
E112	E2032	C24	4.50	5.50
E112	E2032	C26	5.49	6.71
S115	S2035	C22	3.24	3.96
S115	S2035	C24	4.05	4.95
S115	S2035	C20	4.41	5.39
S115	S2035	C27	4.14	5.06
S115	S2035	C29	4.77	5.83
R116	R2036	C24	6.66	8.14
R116	R2036	C27	5.31	6.49
R116	R2036	C29	6.84	8.36
F119	F2039	C28	5.04	6.16
F119	F2039	C33	4.95	6.05
F119	F2039	C35	4.41	5.39
F119	F2039	C39	5.13	6.27
F119	F2039	C41	6.39	7.81

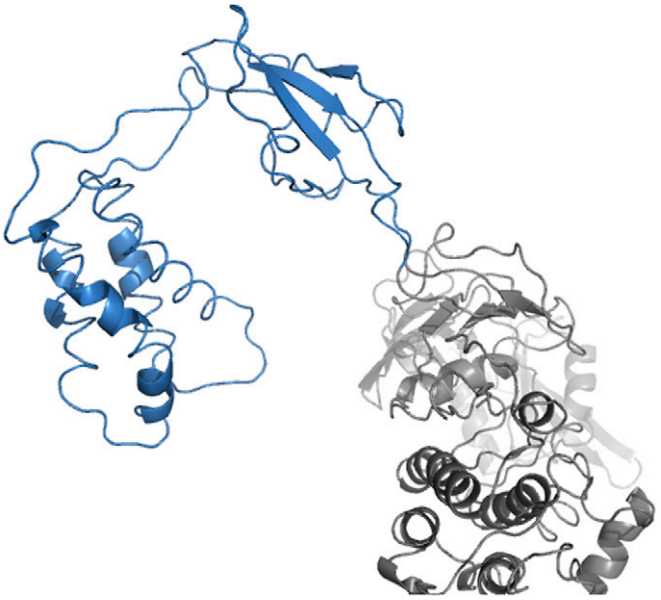

Movie S1. Subdomains of uniRapR do not bind to each other in the absence of rapamycin. Molecular dynamics simulation demonstrates free movement of the uniRapR (blue) inserted into the catalytic domain of Src kinase (gray). The simulations were performed as described in *Materials and Methods*.

Movie S1

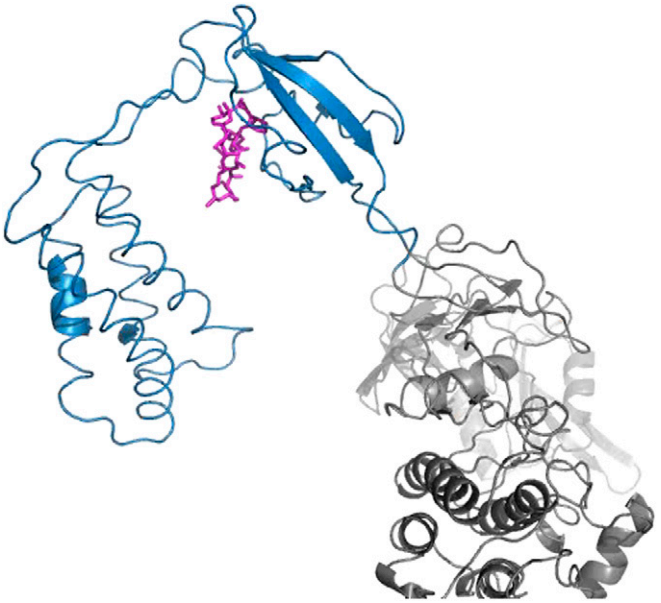

Movie S2. Subdomains of uniRapR do not bind to each other in the presence of rapamycin. Molecular dynamics simulation demonstrates binding of uniRapR subdomains (blue) inserted into the catalytic domain of Src kinase (gray) in the presence of rapamycin (magenta). The simulations were performed as described in *Materials and Methods*.

Movie S2

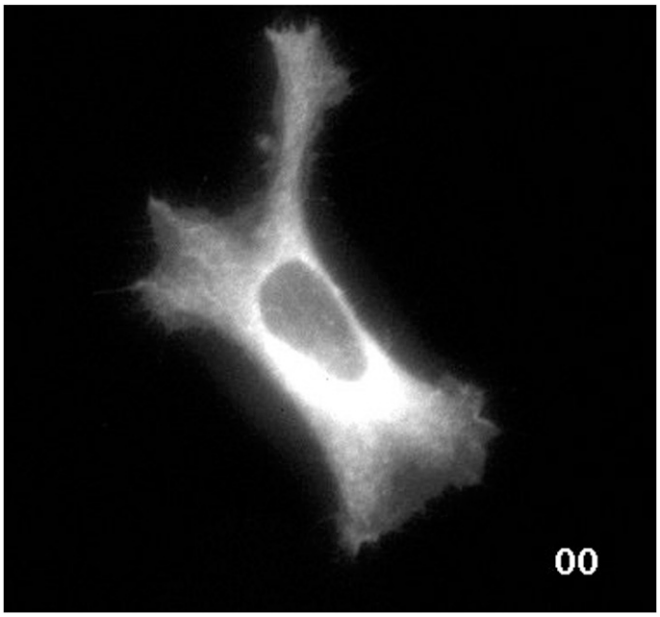

Movie S3. Spreading of HeLa cells upon temporal activation of Src with uniRapR shown with fluorescent imaging. HeLa cells transfected with mCerulean-uniRapR-Src (YF) were filmed for 30 min before and 60 min after addition of rapamycin. Fluorescent images were taken at 1-min intervals.

Movie S3

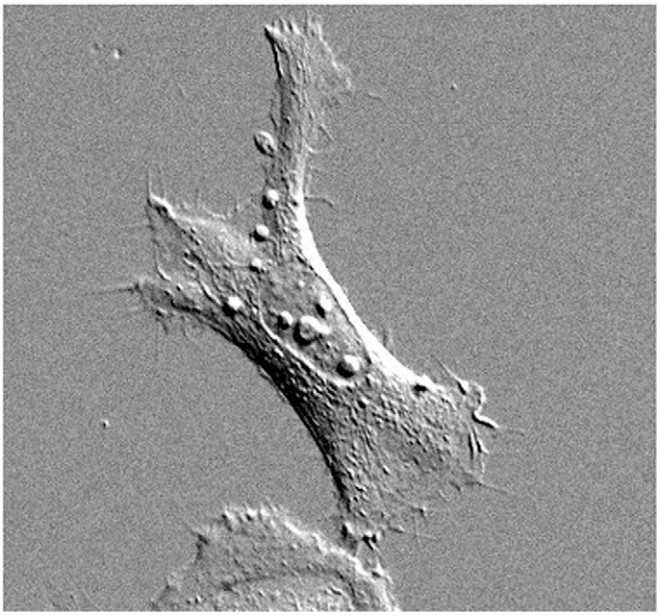

Movie S4. Spreading of HeLa cells upon temporal activation of Src with uniRapR shown with DIC imaging. HeLa cells transfected with mCerulean-uniRapR-Src (YF) and were filmed for 30 min before and 60 min after addition of rapamycin. DIC images were taken at 1-min intervals.

Movie S4